Earth-Science Reviews 154 (2016) 14–28

Contents lists available at ScienceDirect

Earth-Science Reviews

journal homepage: www.elsevier.com/locate/earscirev

Fault linkage and relay structures in extensional settings—A review

Haakon Fossen [a,b], Atle Rotevatn [a]

[a] Department of Earth Science, University of Bergen, Allégaten 41, N-5007 Bergen, Norway
[b] Museum of Natural History, University of Bergen, Allégaten 41, 7800, N-5020 Bergen, Norway

ARTICLE INFO

Article history:
Received 31 July 2013
Received in revised form 21 November 2015
Accepted 23 November 2015
Available online 24 November 2015

Keywords:
Relay structures
Relay ramps
Fault growth
Fault interaction
Fault stepovers

ABSTRACT

Normal fault relay structures form at all scales as faults interact or step out of their own plane during growth, and their successive formation and destruction represent the most efficient way for faults to lengthen. Their progressive evolution from the moment of fault overlap to a fully breached fault involves strain accumulation in the fault overlap zone, initially through bending of layers and secondarily by the formation of fractures, deformation bands (porous sandstones) and subsidiary faults. These small-scale structures have more complex orientation patterns than the typically strike-parallel orientations seen in ordinary damage zones away from sites of fault interaction. Breaching occurs at a given level of bending (dip or curvature) and at the achievement of a critical level of fracture or deformation band density that again depends on local geometric and lithologic/mechanical conditions, but a ramp slope close to 10–15° at the onset of breaching seems to be common. Relay zones are not only lateral communication paths for fluid flow across sealing faults, but their anomalously wide and well-developed damage zones make them conduits of vertical fluid flow in petroleum, groundwater, CO_2 sequestration and magma settings alike, and therefore also serve as sites of ore deposits.

Contents

1. Introduction

Relay and transfer structures are locations of fault interaction where strain or displacement is transferred or relayed from one structure to another (Figs. 1 and 2). They allow individual faults to have finite lengths and thus along-strike strain- or displacement variations, while the system as a whole (for example a rift) acts as a coherent system that maintains a laterally constant amount of extensional strain as measured across the rift (e.g., Walsh and Watterson, 1991). Relays and transfer structures occur in many settings and scales in naturally deforming rocks where populations of structures evolve from small to large sizes. In the most general sense this includes the formation and growth of fold populations as well as the development of fracture, vein and fault populations in any tectonic regime. However, modern use is generally restricted to faults, and this paper will focus on normal fault relay zones, although most of the characteristics easily translate into other regimes and settings (e.g., Nicol et al., 2002).

Dahlstrom (1969) realized that displacement on thrust faults in the Canadian Rocky Mountains varies along the faults, and found that as displacement tapered out along one thrust fault it was commonly

http://dx.doi.org/10.1016/j.earscirev.2015.11.014

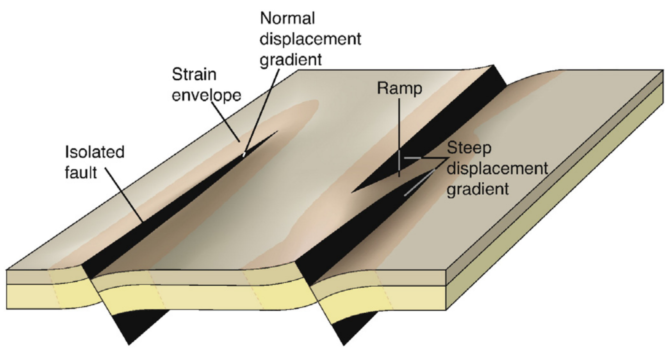

Fig. 1. Normal fault relay structure with a ramp connecting the hanging wall and footwall, showing how relay ramps form when the faults are close and their two strain envelopes overlap (right). An isolated fault is shown in the left part of the figure.

being relayed to an adjacent and overlapping subparallel thrust. Dahlstrom (1969, p. 752) described this as “a kind of lap joint wherein the fault whose displacement is diminishing is replaced by an échelon fault whose displacement is increasing”. He referred to such thrust-fault relay structures as transfer zones, and realized that they occurred along faults that were connected at depth by means of a basal décollement.

The terms transfer zone and accommodation zone were later used about extensional structures by a number of authors (e.g. Bosworth, 1985, 1987; Rosendahl et al., 1986; Morley et al., 1990; Gawthorpe and Hurst, 1993) for zones separating large (typically 100-km scale) structural domains of different characteristic fault architecture or dip directions. They transfer fault strain from one side of the rift to the other, and classical models for transfer or accommodation zones exhibit arcuate faults bounding sub-basins (half-grabens) in rift systems, primarily the East African rift system. They were commonly portrayed together with low-angle detachments in the 1980s and 90s (e.g., Bosworth, 1985; Faulds and Varga, 1998), in many cases more as a result of the strong focus on low-angle extensional detachments and listric faults at the time (e.g., Gibbs, 1984; Wernicke and Burchfiel, 1982) than from objective observations based on hard geologic or geophysical data. However, in many cases transfer zones are not related to low-angle detachments, and they do not have to involve markedly curved master faults. Furthermore, transfer zones are first-order relay structures in rift systems that also host secondary relay structures that are important both from a structural and petroleum geology perspective. Hence, while transfer zones technically are major *relay zones* that involve a number of faults and smaller structures, the term *relay structure* is used about simpler structures involving two (master)faults whose fault tips are interacting. Consequently a transfer zone typically contains a number of relay structures, which is evident from the examples portrayed in Fig. 3.

Even though the geologic term relay structure had been in sporadic use for decades (e.g., Goguel, 1952), the term did not catch on until it was explained and nicely illustrated by Larsen (1988) based on his mapping of an extensional fault array in the Permian of East Greenland. Since then, the term has for the most part been used about fault interaction structures in extensional settings (e.g., Peacock and Sanderson, 1991; Willemse, 1997; Crider and Pollard, 1998). In such settings, and in particular with respect to petroleum geology and fluid flow, relay structures are particularly important as they occur in large numbers in rifts and faulted continental margins (e.g., Anders and Schlische, 1994; Young et al., 2001; Jackson et al., 2002; Bense and Baalen, 2004; Elliott et al., 2011). Relay structures are also important with respect to drainage patterns and facies variations along active faults that breach the surface (Gawthorpe and Leeder, 2000; Athmer et al., 2010). In particular, they focus sediment supply to local hanging-wall depocenters. There has also been a recent interest in the damage (in most cases structures below seismic resolution) associated with relay structures, both in the context of fluid flow in petroleum and hydro reservoirs (Fossen et al., 2005; Rotevatn et al., 2007), ore mineralization (Cox, 2005; Xiao-shuang et al., 2005), hydrothermal systems (Faulds et al., 2013) and, for large relay structures, the control that strain-hardened relays may have on rupture propagation during earthquakes (Manighetti et al., 2009; Finzi and Langer, 2012).

In this review we will look at relay structures in normal fault populations. Although oppositely dipping fault interaction structures are also regarded as relay structures (Morley et al., 1990), we only discuss such arrangements in terms of large transfer or accommodation zones. For simpler relay structures we limit our review to structures forming by interaction between (sub)parallel fault segments. We review important geometric and evolutionary aspects of fault relay zones in extensional fault systems and discuss their implications for fluid flow.

Fig. 2. Relay structure in Canyonlands National Park (Devils Lane) showing rapid fault displacement fallof (unusually high displacement gradient) toward the tip. The ramp itself contains several faulted joints.

2. Linked fault systems

The evolution of large fault structures occurs by one or a combination of the following mechanisms: (1) simple tip propagation and coalescence or linkage of initially isolated, smaller fault segments ('segment growth and linkage', sensu Trudgill and Cartwright, 1994; or 'isolated fault growth', sensu Walsh et al., 2003); or (2) rapid establishment of the full length of the fault and subsequent displacement accrual without significant tip propagation ('coherent fault growth', sensu Walsh et al., 2003). Although the two may be seen as competing models to explain fault evolution, it is our view that these represent end-member models for fault growth that are equally applicable in nature, probably even within the same region or rift.

Isolated fault growth occurs with the development of long faults from a population of more or less randomly distributed embryonic faults nucleating from distributed natural heterogeneities in a lithologic unit (e.g., Cowie et al., 2000; Soliva and Schultz, 2008; Fig. 4a). Experimentally this setting is produced in a sandbox experiment where sand is overlying a relatively homogeneously deforming material such as silica gel or basal rubber membrane (e.g., McClay and Ellis, 1987; Vendeville et al., 1987; Vendeville and Cobbold, 1988; Wu et al., 2015). As natural examples we could envisage a system comprising a competent unit (sandstone, limestone, basalt layer) overlying a softer or viscous unit (shale or salt) (e.g., Trudgill and Cartwright, 1994) or clastic sediments sliding on a low-angle décollement of evaporites or overpressured shale on a passive margin (Duval et al., 1992; Fort et al., 2004; Rouby et al., 2011). Numerical models of such settings have shown that fault linkage occurs as the embryonic fault structures grow and interact (Cowie et al., 2000; Allken et al., 2013). Hence the isolated fault growth model requires boundary conditions that distribute strain homogeneously enough for individual and isolated faults to nucleate in a relatively wide area.

The other end-member model, represented by the coherent fault model, is the development of a long fault structure above a buried fault undergoing reactivation (e.g., Giba et al., 2012) (Fig. 4b). Slip on this fault imposes a strongly non-uniform extension with strain localizing in the cover above the fault, and the overall fault propagation is upwards from the reactivated fault. In general the overall upward propagation of basement faults through sedimentary cover tends to generate tip line bifurcation and thus segmented fault systems that link up as strain accumulates (e.g., fig. 8a in Childs et al., 2009). In detail, mechanical stratification may complicate the growth history. For instance, faults may initiate in strong layers above the basement fault and develop into en-échelon faults that then propagate and interact laterally as well as vertically (e.g., Jackson and Rotevatn, 2013).

Varieties of this model occur when the direction of least compressive stress (σ_3) is oblique to the strike of the underlying basement faults, which produces shear displacements along these structures. Depending on the angular relations the fault array in the cover will tend to consist of individual segments that align with respect to the current stress field (perpendicular to σ_3) while the trend of the zone follows that of the basement fault (Fig. 4c). Excellent examples of such developments are found in active volcanic areas such as Hawaii and Iceland (e.g., Acocella et al., 2000; Tentler and Mazzoli, 2005; Podolsky and Roberts, 2008) as well as in rifts and continental margins (Giba et al., 2012; Jackson and Rotevatn, 2013). Whether or not reactivation happens depends on the orientation of preexisting faults relative to the new stress field and on the strength of those faults (Bott, 1959), hence the contribution of each of these processes will depend on local factors. In both cases, linked fault systems form where individual segments interact and link up by relay formation and breaching. The result of such a linkage process is to form a longer fault from several individual small faults.

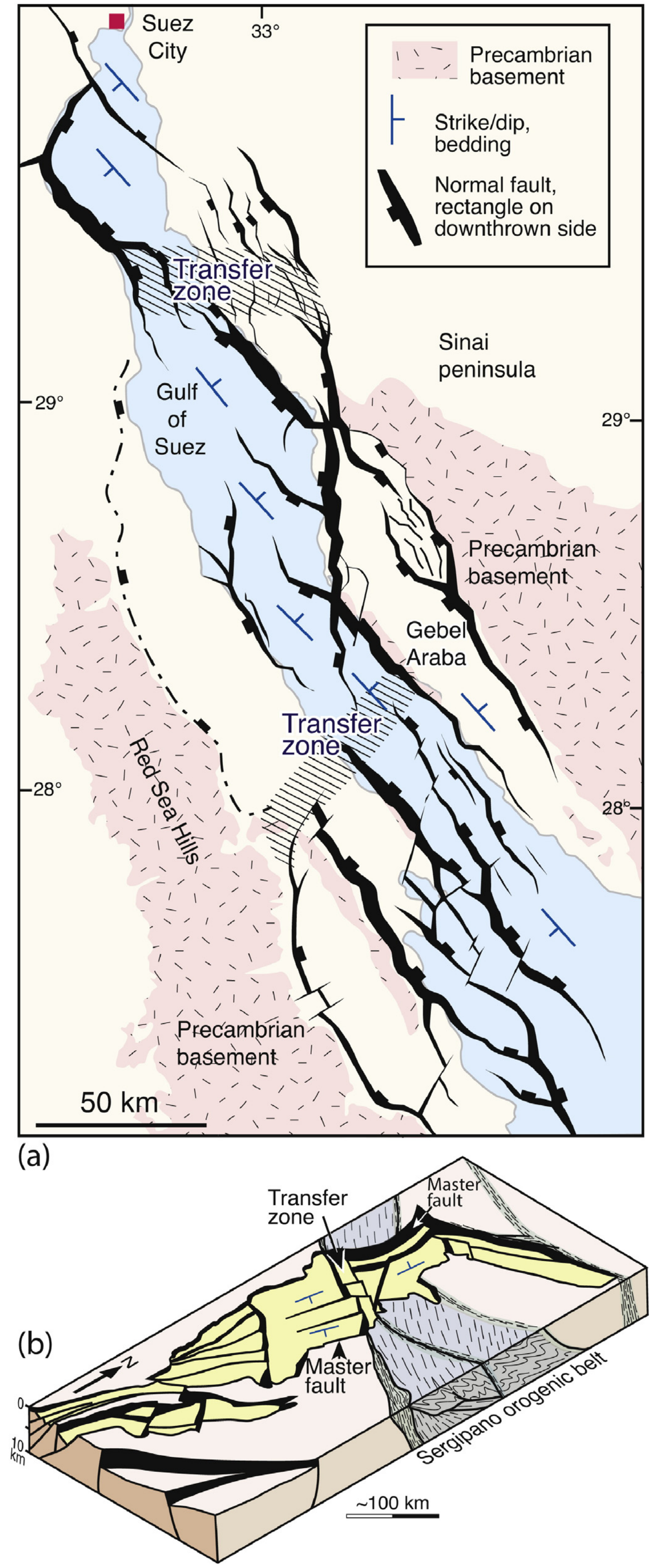

Fig. 3. a) Structural map of the Suez rift, Egypt. Based on Bosworth (2015). b) 3D model of the Cretaceous Tucano Rift, showing the trend of the Sergipano orogenic belt in the Proterozoic basement and its connection to a transfer zone in the basin. Modified from Milani and Davison (1988).

3. Fault interaction

The likelihood that faults in a given fault population will interact depends not solely on strain, but also on a number of other factors, such as fault density, fault distribution and spatial arrangement of faults in the fault population, the number of faults that grow relative to those that become inactive, and the size of the elastic strain field or stress

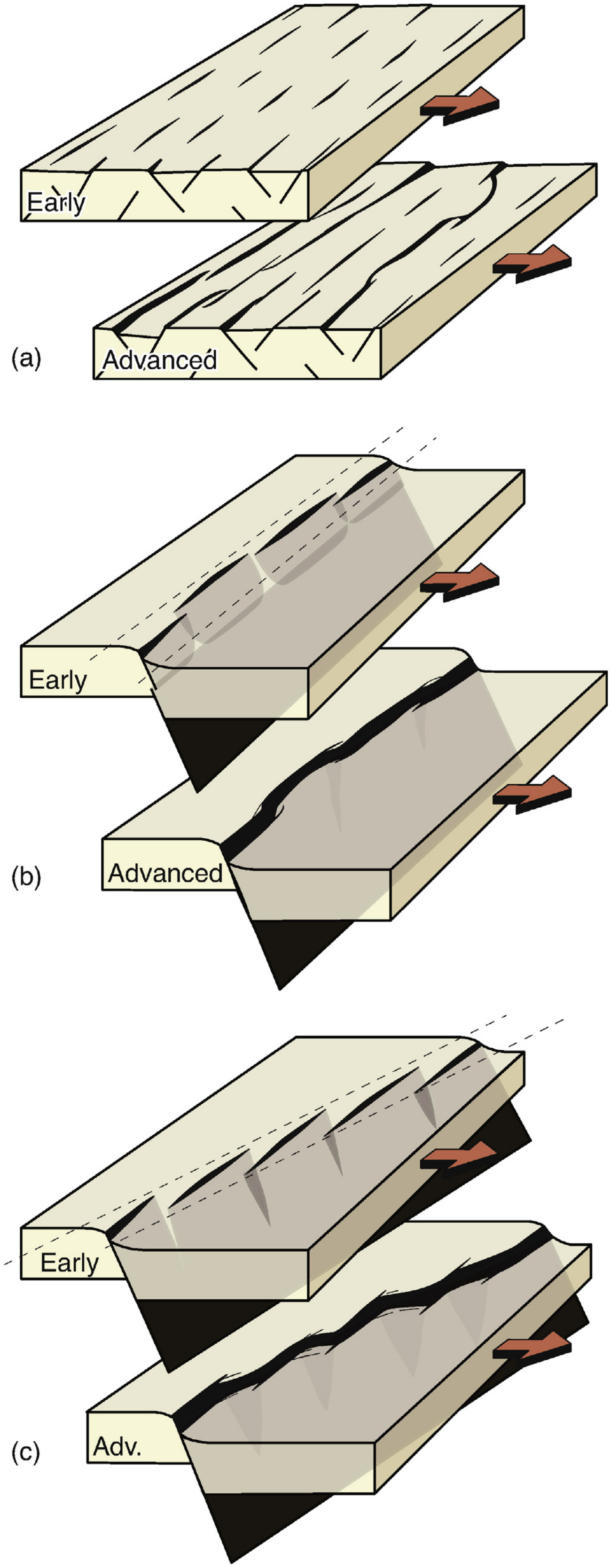

Fig. 4. a) Uniform extension generating a population of incipient faults of which some grow, interact and link up to longer faults. b) Basement-controlled extension generating en-échelon faults in the cover that link up to a non-planar large fault. c) Variation of b) where the preexisting fault is inclined with respect to the extension direction.

perturbation around the faults (Cowie et al., 2000; Walsh et al., 2003; Soliva et al., 2006). However, it also depends on whether the available faults are more or less randomly distributed throughout the volume of deforming rocks (e.g. a magmatic rift zone) or whether fault segmentation is a consequence of complex vertical propagation of deeper structures (Soliva and Schultz, 2008), similar to the twisted geometry of dike fringes described repeatedly through the literature on dike intrusion geometry (e.g., Anderson, 1951; Delaney and Pollard, 1981) (Fig. 4c). The boundary conditions for the area or volume of rock undergoing faulting are important factors in this respect.

3.1. The role of boundary conditions

The overall distribution or arrangement of faults in the population is controlled by kinematic boundary conditions as well as rheology and mechanical layer properties. By kinematic boundary conditions we mean the external causes and controls on the type (plane versus three-dimensional strain, strain rate) and magnitude of strain in the deforming volume of sediments or rocks. Boundary conditions are easier to visualize for physical models such as sand box experiments, namely the base (flat, irregular, stretching rubber sheet, etc.) and walls (fixed or moving). In nature, the base of a deformed sedimentary sequence or basin can be a detachment or salt layer, or heterogeneous with mechanically weak preexisting faults and fabrics whose location, orientation and arrangement will potentially influence the structures and their distribution in the overburden (e.g., Fig. 4b–c).

3.2. Preexisting structures

Preexisting faults and fabrics in the basement of regions undergoing extension may or may not influence the formation and localization of transfer structures or relays. In general, it is the largest structures that are influenced by basement anisotropy, and although transfer zones can develop in the absence of basement structures (Schlische and Withjack, 2009), a close correlation between basement structures and transfer zones has been reported for a number of rifts worldwide. For instance, the East African Rift is influenced both by a steep metamorphic basement fabric and ductile/brittle basement shear zones that were reactivated during rifting, locally with the formation of pseudotachylite (Hetzel and Strecker, 1994; Smith and Mosley, 1993; Kinabo et al., 2007). Similarly, the geometry of the Tucano Rift in NE Brazil is influenced by the oblique fabrics and faults of the Sergipano orogenic belt (Fig. 3b), which guided the establishment of an oblique transfer zone and an associated change in fault polarity (Milani and Davison, 1988; Destro et al., 2003). The Suez-Red Sea Rift (Fig. 3a) is yet another example where the locations and orientations of transfer or accommodation zones relate to basement structures (Younes and McClay, 2002). In the last two examples many of the masterfaults are, on average, fairly straight, as opposed to the curved geometries presented schematically in early works on accommodation and transfer zones (e.g., Rosendahl et al., 1986).

The strong influence of preexisting basement structures on first-order transfer zones where strain is relayed from one side of the rift to the other makes these structures different from smaller-scale relay structures that may have little or no inheritance. Many, if not most rift transfer zones are directly dictated by reactivating oblique basement structures, whereas smaller relay structures form as the result of local stress interaction between overlapping fault tips. However, the location of such interacting faults may well be influenced by preexisting structures, in which case there is an indirect influence by preexisting structures. In general, the study of both relay structures and transfer zones should involve a structural study of the basement itself if possible.

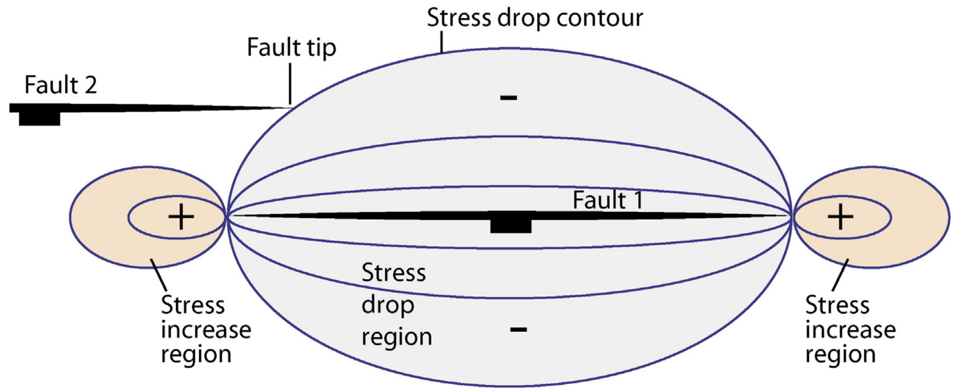

Fig. 5. Zones of stress drop/increase around a normal fault (Fault 1). The growth rate of an overlapping fault tip (Fault 2) would be retarded as the tip enters the stress drop region of the adjacent fault (Fault 1).

3.3. The process of linkage: relay ramp formation

Once two subparallel fault segments get close enough they will start to interact (Fig. 1). This is manifested by the retardation or temporal arrest of the fault tips, the curving of fault tips in the overlap zone, the development of a complex zone of subsidiary structures (faults, fractures, deformation bands) and the formation of a ramp. The ramp is a result of the steep displacement gradients that develop in the fault overlap region (Peacock and Sanderson, 1991; Nicol et al., 1996), implying that the interaction of fault tips slows down the propagation rate of the tips involved (e.g., Maerten et al., 1999). Furthermore, a high displacement gradient in the fault tip regions accentuates the ramp that forms between the two overlapping segments, whose dip direction is controlled by the arrangement and kinematics of the faults.

The critical nearness or spacing at which two fault tips interact is of importance in understanding fault tip interaction during the growth history of fault populations. Mechanically, this critical spacing has been related to the zone of stress reduction that occurs around faults (e.g., Ackermann and Schlische, 1997; Cowie and Roberts, 2001; Soliva et al., 2006) (Fig. 5). The effect of such a stress drop region has been explored by Willemse et al. (1996) and further by Gupta and Scholz (2000), whose modeling confirmed that tip propagation is retarded as a fault grows into the stress drop region of an overlapping fault. The consequence of this reduction in propagation rate is the aforementioned development of a skewed displacement profile, with an average gradient toward the overlap region that is up to 2.5 times that of isolated fault tips (e.g., Soliva and Benedicto, 2004). The steepening of the displacement gradient profile elevates the stress concentration at the tip, which drives the fault to propagate into the stress drop region of the overlapping fault, but at some critical stress drop value, propagation stops. The result is a (soft-linked) relay ramp or, if strain continues to be accommodated by the fault system, a breached relay (hard-link; see next section) (Walsh and Watterson, 1991) (Fig. 6). If the two tips propagate simultaneously, both tip gradients steepen as the tips are influenced by each other's stress drop zone.

The critical spacing of faults, above which they do not interact, is related to fault length and fault displacement; large faults have a wider stress perturbation zone than small faults and thus interact with faults that are farther away. This leads to a well-defined relationship between relay width and relay length (fault overlap) that is constant over a wide range of fault sizes (Fig. 7). Soliva et al. (2006) demonstrate that relay width can be related to mechanical layer thickness. In particular, observations indicate a characteristic spacing of ~0.5 times the layer thickness over a wide range of scales (Fig. 15 in Soliva et al. (2006). This ratio is influenced by site-specific factors such as local fault geometry, fault weakness, rock properties, and preexisting weak structures, which together contribute to the scatter in the data of about two orders of magnitude (Fig. 7). In the crust, mechanical layering occurs at a range of scales from bed or lamina thickness to the thickness of the brittle crust. For a thickness of the brittle crust of 10–12 km, a spacing of major extension faults in rift could be expected to be around 5 km, which could produce first-order relay structures with a characteristic width of ~5–6 km. Others use the elastic thickness of the lithosphere to model the spacing (e.g., Spadini and Podladchikov, 1996). Morellato et al. (2003) found that many rifts show a characteristic major fault spacing of 4–6 km, while other rifts show larger characteristic spacing (up to 30 km). Hence, individual relay ramps more than 30 km wide are observed in rifts, and in extreme cases the width can get close to 100 km (Peacock et al., 2000).

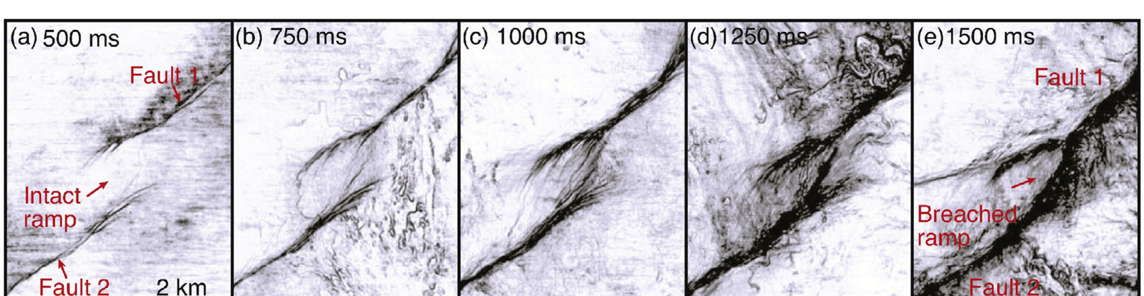

Fig. 6. Seismic data (variance timeslices) showing two overlapping faults forming a relay ramp (a) that becomes breached at depth. At 1500 ms (two-way time) the ramp is completely breached (hard-linked). Modified from Giba et al. (2012).

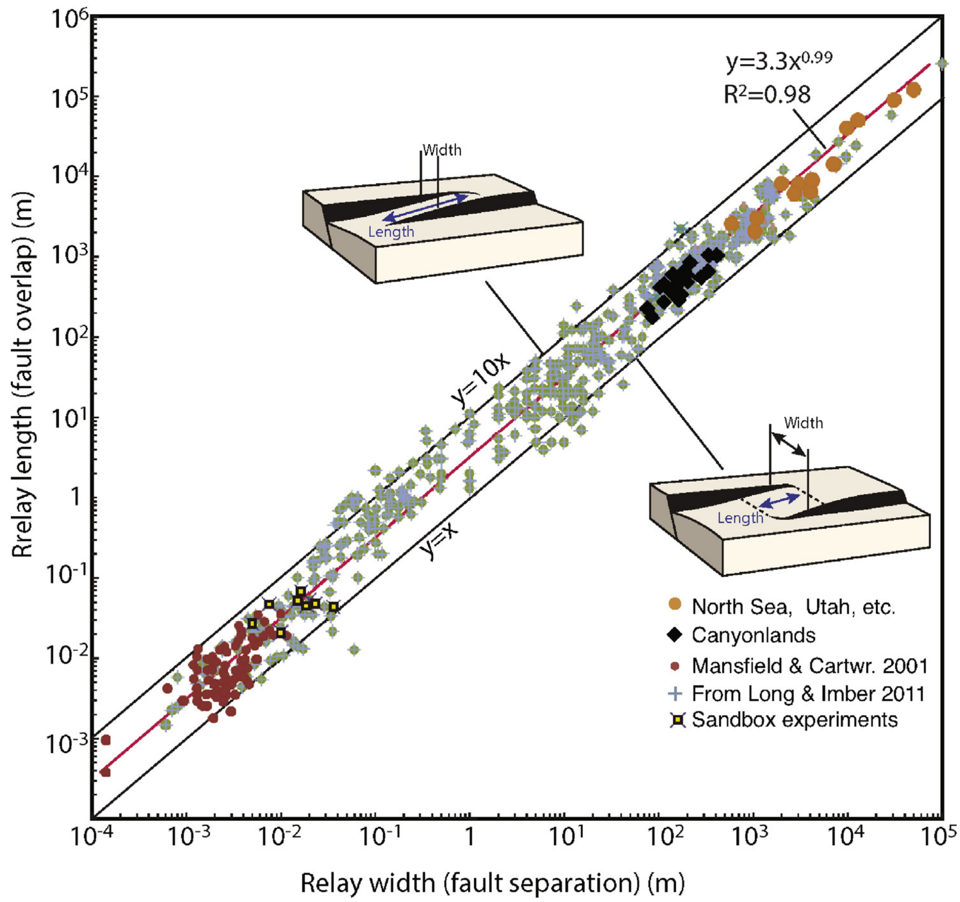

Fig. 7. Relationship between relay width and relay length (fault overlap). Data from Long and Imber's (2011) compilation, various other sources and own data. Regardless of size, ramp length is on average 3–3.5 times their width.

3.4. The breaching of relay ramps

As faults overlap and the relay structure is established, the ramp will deform internally and breaching will eventually occur if strain keeps accumulating. The deformation structures that form within evolving relay structures depend greatly on the mechanical rock properties at the time of deformation. Soft clastic sediments at shallow depths will most likely deform by non-cataclastic granular flow that over time may localize into shear bands that may or may not involve strain hardening (e.g., Antonellini et al., 1994; Kristensen et al., 2013). Sandstones (as opposed to unlithified sand) are more likely to develop cataclastic deformation bands that lead to strain hardening in the ramp and eventually to faulting (Aydin et al., 2006; Fossen et al., 2007). For lithologies that develop fractures rather than deformation bands, such as well-indurated siliciclastic sediments (like the Canyonlands example; Fig. 2) and most limestones, effective strain weakening occurs and the breaching fault may establish itself along fracture zones.

Several factors dictate the onset of breaching. One is the mechanical properties of the material within the relay zone. Soft materials such as poorly consolidated siliciclastic sedimentary layers would be expected to accommodate more flexing prior to breaching than stiffer rocks such as well-indurated sandstone, limestone, basalt or basement rocks. A familiar exception is the probably still active Canyonlands National Park example, where relays are forming at the surface in quite stiff Permian sandstones. In this case the fractures open in tension and then shear (slipped fractures) so that the evolving ramp consists of a number of extension fractures running across and along the ramp (Fig. 2). Hence some ramps reach maximum dips as high as 26° (Fossen et al., 2010) or perhaps 30° (Trudgill and Cartwright, 1994) in the Grabens area of Canyonlands National Park. We expect that ramps in such stiff layers would breach at lower dip angles at burial depths of >1 km.

Giba et al. (2012) presented illustrative seismic data from a relay ramp offshore New Zealand (Fig. 6) that developed by reactivation of an older fault similar to the situation portrayed in Fig. 4c. Because sedimentation occurred durig fault growth, we can see a progressively more mature ramp as we move stratigraphically downward through the synrift sequence, and hence an evolution from an unbreached to a breached relay structure, as illustrated in Fig. 6. Giba et al. (2012) also demonstrate that the ramp becomes steeper downwards as strain increases, and becomes breached as the maximum dip of the ramp reaches around 13–14°. Breaching (or yield) criteria, such as the critical amount of dip or curvature of layers in the relay ramp, is potentially useful for predicting subseismic breaching faults from seismic interpretations. The limited amount of ramp dip data shown in Fig. 8 supports the idea that unbreached ramps have lower dips than barely breached ramps, and that well-breached ramps display the largest dips. The latter may indicate that some ramps keep steepening also during the breaching process, although relaxation may also be expected, creating a particularly wide range of dips for well-breached ramps. Clearly, the critical dip depends on the material properties of the layers in the ramp (notably layer stiffness), and also on the local state of stress in the perturbed stress field between the overlapping fault tips (Fig. 5), both of which are related to burial depth, fault geometry, lithology and diagenetic history.

There is always a component of lengthening of the layers within the ramp as they bend, as controlled by the ramp geometry (Ferrill and Morris, 2001). Additionally, there is a component of twisting of

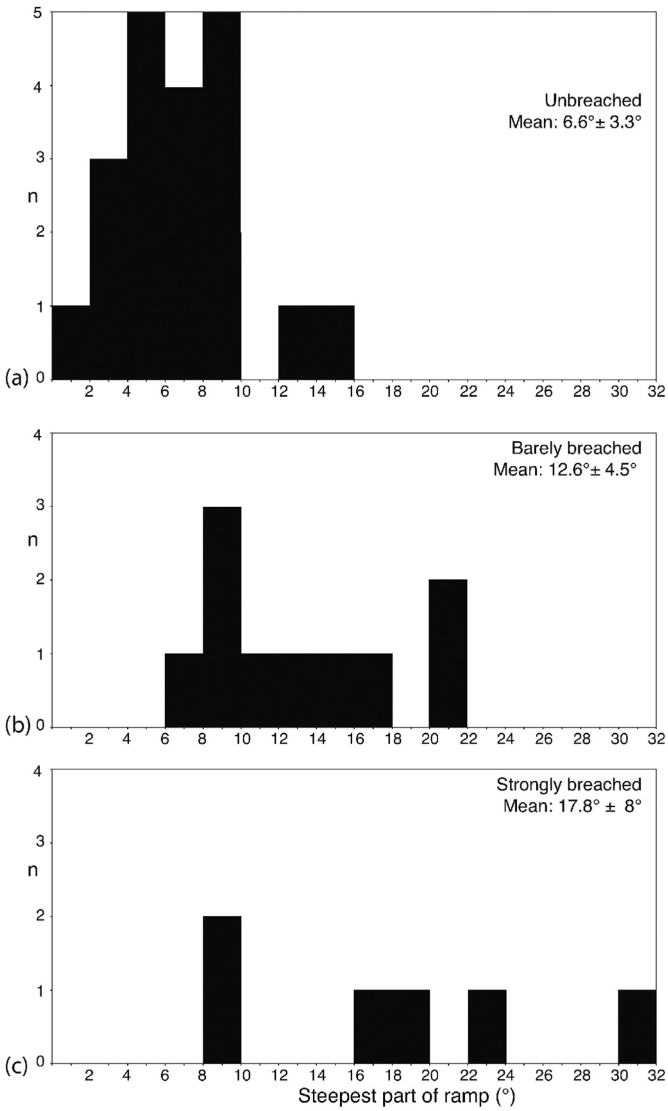

Fig. 8. Distribution of maximum dip of relay ramps that are a) unbreached, b) barely breached, and c) well breached. Outcrop-based data from Soliva and Benedicto (2004); Huggins et al. (1995); Xu et al. (2011); Rotevatn and Bastesen (2012); Giba et al. (2012), and Bastesen and Rotevatn (2012). Dip is relative to the general (regional) layer orientation.

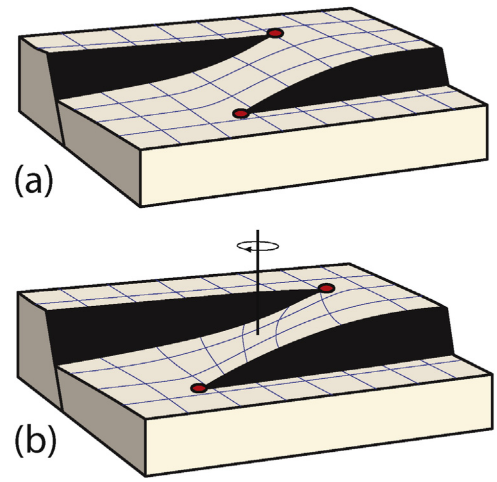

Fig. 9. The twisting of a relay ramp as the two overlapping fault tips propagate and the relay lengthens prior to breaching.

the layers in the ramp that develops as the fault overlap increases (Fig. 9)—an effect that is most prominent for steep tip displacement gradients. The stress and strain development within a ramp are also influenced by displacement profiles on the two faults, any non-parallelism or non-planarity of fault tips, and relative growth rates, which makes it difficult to predict detailed stress, strain and fracture patterns within ramps.

There are, in principal, three end-member classes of breached ramp geometries that can be observed from field observations, seismic data interpretation, physical experiments and numerical models (Fig. 10), forming by 1) single-tip breaching, 2) double-tip breaching, and 3) mid-ramp breaching (Fig. 10). Single-tip breaching can be explained by one fault tip being arrested or retarded while the other tip is bending and eventually connecting with the other fault. This results in a curved shape of the connecting fault in map view. If the upper (hanging-wall) fault tip is the one that connects (upper ramp breach), as shown in Fig. 10b, the ramp is preserved in the footwall, which in a petroleum setting could mean a trap if the ramp is large enough. In the case where both faults propagate and connect, the result becomes a lenticular relay zone (Fig. 10c), and displacement may be evenly or unevenly distributed between the two faults. During continued accumulation of displacement, this process results in a fault lens in map view and a fault splay in cross-section. The Delicate Arch ramp (Fig. 11a) is an example of an unbreached ramp where the orientation and distribution of deformation bands in the ramp suggest that an upper-ramp breach (Fig. 10b) was about to be established (Rotevatn et al., 2007). The Peter Creek Ramp in Oregon, described by Crider and Pollard (1998) (their fig. 4) is similar example where a zone of elevated fracture density connects one of the fault tips with the other fault. In contrast, the Canyonlands fault array seems to favor mid-ramp breaching (Fig. 10d). The reason for this difference is probably the brittle nature of the Canyonlands strata and the pre-existing fractures that get reactivated. Soliva and Benedicto (2004) show small-scale examples of this from limestones in the Pyrenees, and also some hybrid examples of types 2 and 3. A large-scale example of a mid-ramp breach from silisiclastic sedimentary strata in the North Sea is shown in Fig. 11b. In general, the way that a ramp breaches is likely to be a consequence of geometric irregularities of the overlapping faults and lateral variations in fault strength.

Crider and Pollard (1998) modelled ramp evolution numerically and found a concentration of Coulomb stress that bridges the two fault tips in the relay zone. A breaching fault is expected to form in this region of high stress values, and their idealized model predicts breaching in the middle to upper part of the relay ramp (the range between Figs. 10b and d). Crider and Pollard's (1998) model also suggest an irregular or zigzagged composite bridging fault. The Grabens fault array in Canyonlands National Park also does (Cartwright and Mansfield, 1998), but may not be representative for other and more common fault populations for reasons mentioned above. In general, more detailed observations are needed for a statistical evaluation of these characteristics. The general picture is that within each fault array or faulted region a wide range of geometries are observed, typically with representation of all cases shown in Fig. 10 (see examples in Soliva and Benedicto, 2004).

It is important to realize that the transition from intact rock to a breached ramp is a gradual one that usually involves the accumulation of small-scale deformation feature such as fractures, deformation bands and minor faults prior to wholesale breaching and fault coalescence. Hence, rocks constituting a ramp will undergo mechanical and petrophysical property changes throughout the evolution toward a fully breached ramp. As ramp-internal structures evolve, the scale-dependent concept of ductility becomes important. For

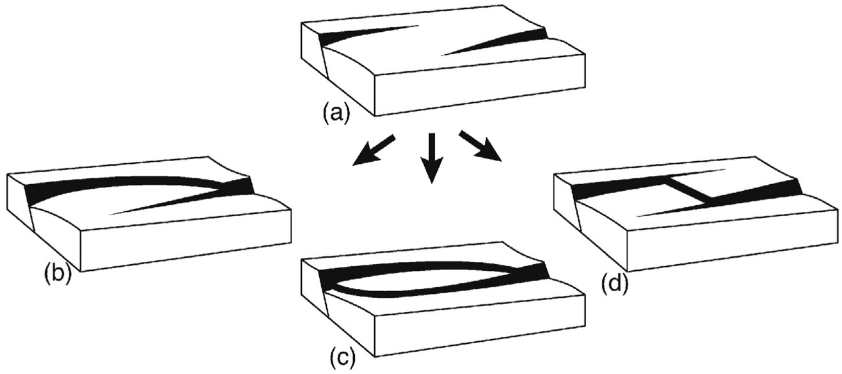

Fig. 10. Patterns of relay ramp breaching. a) Unbreached relay ramp. b) Single-tip (upper-ramp) breach. c) Double breach. d) Mid-ramp breach.

example, what appears continuous and unbreached at the seismic scale may reveal itself as highly deformed at outcrop scale. Another situation is where the overlapping fault tips are too close to be resolved on seismic data, resulting in the interpretation of a map-view kink in the fault interpretation.

Soliva and Benedicto (2004) suggested a criterion (c*) for breaching based on the relationship between relay displacement (D, the sum of fault displacements across the relay) and relay width (fault separation, S) of the form $D = c^*S$, where c^* varies from 1 ($D = S$) to 0.27 ($D = 0.27S$) for relays that show evidence of incipient breaching. Hence c^* is a threshold value that holds for centimeter- to kilometer-scale relays alike, suggesting that relay-forming and -breaching processes are similar over a wide range of scales.

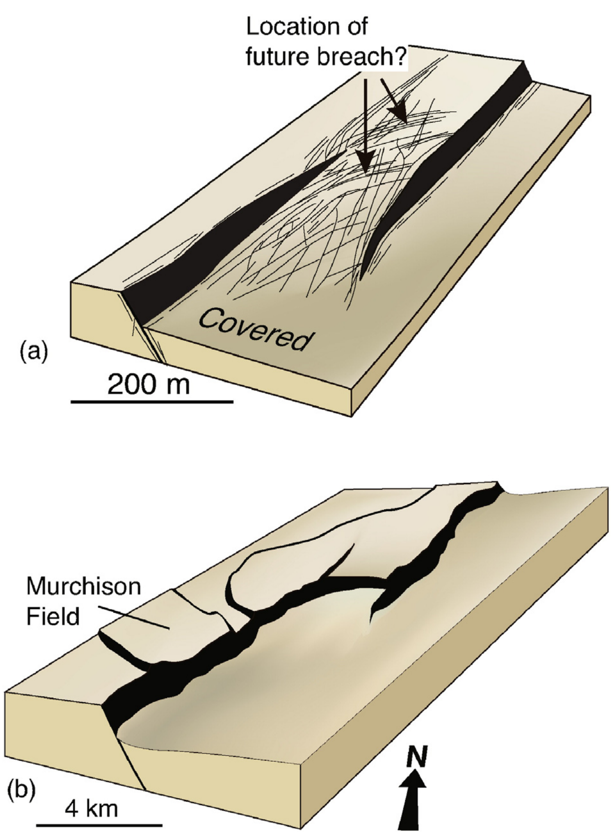

Fig. 11. Relay ramp in (a) Arches National Park (from Rotevatn et al., 2009b) and (b) the North Sea (Murchison Field area, based on Young et al., 2001). The latter example is based on seismic interpretation, hence small (subseismic) structures are not displayed (but can be inferred from a).

The dip and curvature of ramps are directly reflected by the displacement profiles of the two fault segments. In general, observations suggest that most faults involved in relay structures (fault tip interaction) show convex displacement profiles where the gradient increases toward the tip (Fig. 12). This observation implies that the bending of layers is most "forceful" in the tip region. However, some cases show a reduction in displacement gradient close to the tip (in the overlap region; see Soliva and Benedicto (2004) for examples), implying that the curvature of the ramp is higher in the central part of the ramp. Assuming a positive correlation between subseismic fracture and curvature, this geometry favors a central breach (class 3, Fig. 10d). Furthermore, displacement profile types vary within fault populations, indicating that they depend on local geometric or mechanical complications that are difficult to predict.

These geometric characteristics and their variability may have significant influence on depositional patterns where fault linkage occurs near the surface. They may control drainage patterns and the hydrologic conditions in a developing rift basin (Bergner et al., 2009), which again affect the distribution of reservoir-quality deposits and thus are of significant interest during exploration in rifts and continental margins. In simple terms, steeper displacement variations associated with ramp structures enhance their influence on depositional patterns, and more work is needed to investigate the factors influencing such structuring during fault linkage.

3.5. Fault linkage of curved fault segments

Above we considered relay structures defined by overlapping parallel faults. However, even though large faults can be fairly straight (Fig. 3a), particularly where guided by preexisting faults, several fault systems are composed of fault segments that are curved in map view, where the curved segment are interpreted as individual faults that have linked up to a much longer fault system. This pattern is particularly pronounced in large-scale normal fault systems, such as the Wasatch Fault system in Utah (Fig. 13a), and rift systems such as the East African rift system and the North Sea rift system (e.g., Scott and Rosendahl, 1989; Fig. 13b), but occurs on all scales down to cm-scale structures in physical models.

The Wasatch fault (Fig. 13a) is a 370 km long and composite normal fault system composed of ten hard-linked curved segments (Machette et al., 1991), and its characteristic curved geometry is particularly well developed in the Provo-Salt Lake City area (Provo and Salt Lake City segments). Curved geometries seem to be repeated at several scales along this fault complex, but we will here confine ourselves to the first-order structures, defined by ca. 40–50 km long segments with several kilometers of throw. Several of the segment boundaries define salients ("turtle backs") that plunge westward into the Basin and Range extensional province.

Strikingly similar fault geometries of comparable size are seen in the Jurassic sedimentary sequence of the northern North Sea rift system, for

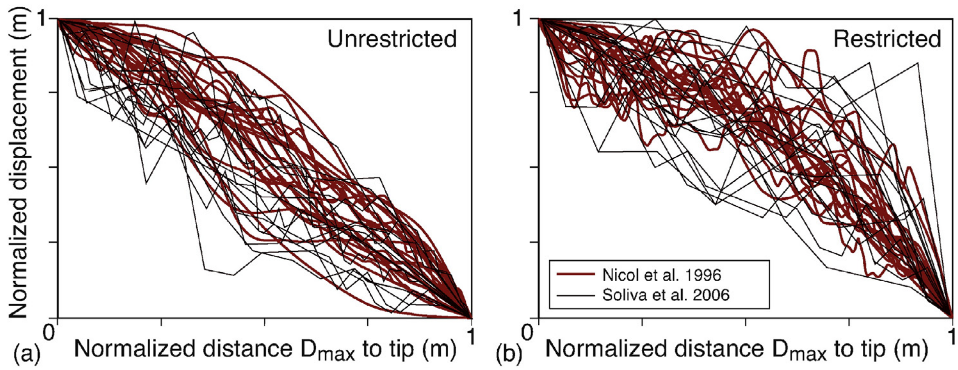

Fig. 12. Displacement variations for a) non-interacting and b) interacting faults, measured from the point of maximum displacement (Dmax) to the fault tip. While non-interacting faults show a close to linear displacement gradient, the more convex shape of the interacting fault data reflect the effect of growth restriction at sites of fault interaction (relays). Data from Nicol et al. (1996) and Soliva et al. (2006).

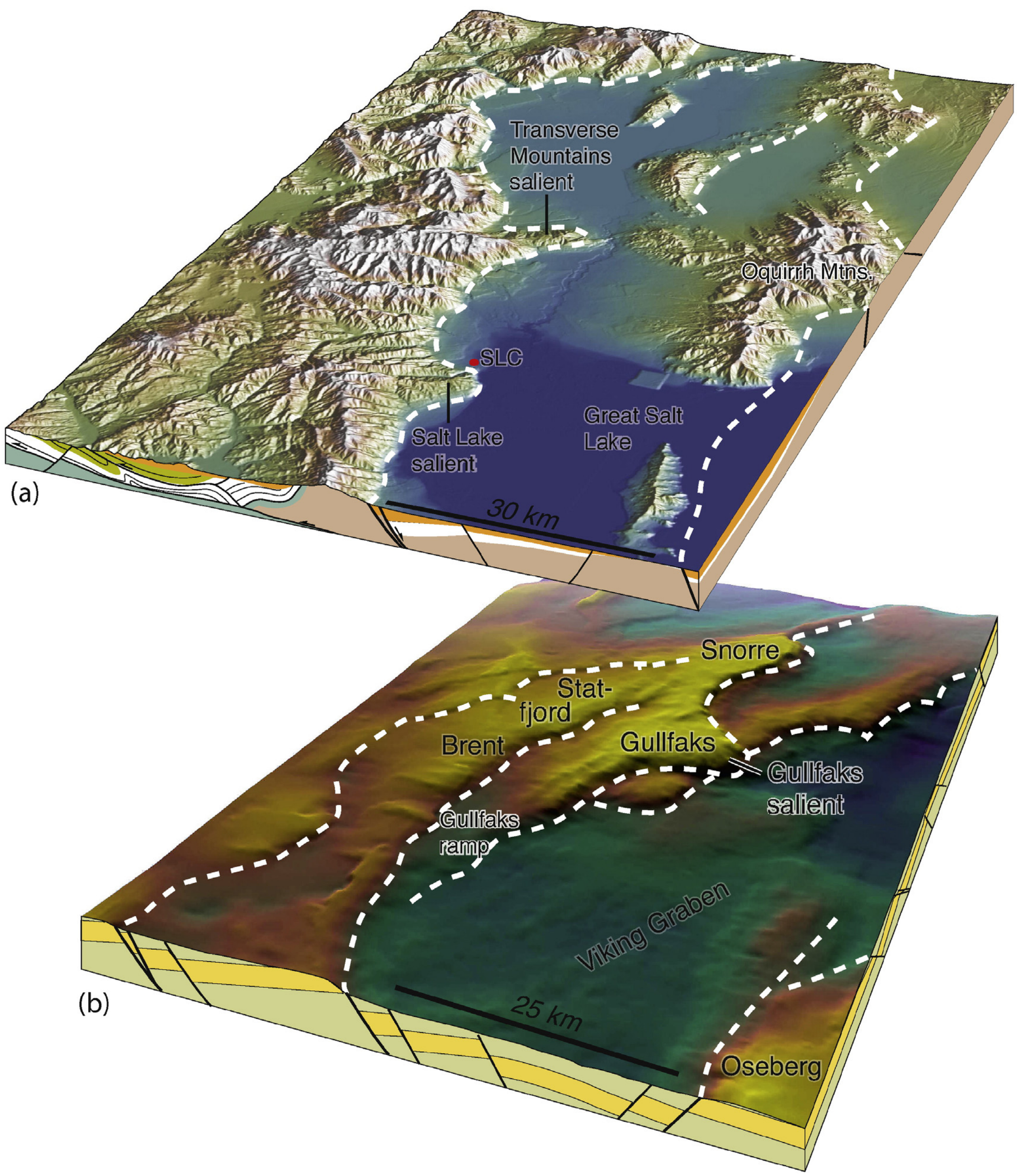

Fig. 13. a) The Wasatch Fault in the Salt Lake area, Utah, portraying a strongly curved fault trace in map view. b) Strikingly similar fault patterns in the northern North Sea (base Cretaceous unconformity). First-order faults with km-scale displacements are indicated (simplified).

first-order faults with km-scale offsets (Fig. 13b) (Fossen et al., 2000). Also in this area the segment boundaries define salients or cusps that point toward the down-faulted hanging wall side, generally toward the rift axis.

There are certain models and conditions that can explain curved fault patterns in map view, although such fault patterns are not always easy to understand. One factor that may be particularly important for large faults, such as the ones mentioned above, is the influence of preexisting heterogeneities, including the reactivation of older faults or fault arrays (Sevier thrusts in the case of the Wasatch Fault) that formed in different stress regime(s). Reactivation of non-planar thrusts is a well-known factor in the Basin and Range province (Coney and Harms, 1984) and reactivation of Permo-Triassic normal faults or Devonian extensional structures was important in the development of the mid-late Jurassic North Sea rift system (Færseth, 1996; Fossen et al., 2000). Preexisting faults can dictate the location of younger faults as well as their orientation and geometry. Interestingly the Wasatch Fault system developed straighter fault segments in some areas, such as the Weber segment north of the Salt Lake segment. At present we do not know the reason for these variations along this particular fault system, but a curved geometry seems to be a common feature of many large-scale extensional faults.

As a first-order approach to the evolution of both the North Sea and Wasatch Fault examples, we suggest that the faults initiated as individual segments whose fault tips at some point interacted at the locations of the salient. This model predicts maximum structural complication and minimum displacement in the areas of fault interaction (i.e., in the salients), and depocenters near the middle of the curved fault segments. Seismically this is consistent with the characteristic earthquake model (Schwartz and Coppersmith, 1984), which for segmented fault systems predicts that large earthquakes with similar (characteristic) size are repeated on individual segments. These characteristics are present in the Salt Lake and Gullfaks areas (Machette et al., 1991; Fossen et al., 2000), and the similarity in both overall fault geometry and presence and location of subsidiary faults within the salients is striking (Fig. 14). For faults with km-scale offsets, gravitational destabilization of elevated footwall salients may add to the tectonically-driven extensional faulting. Hence gravity-influenced crestal collapse may be

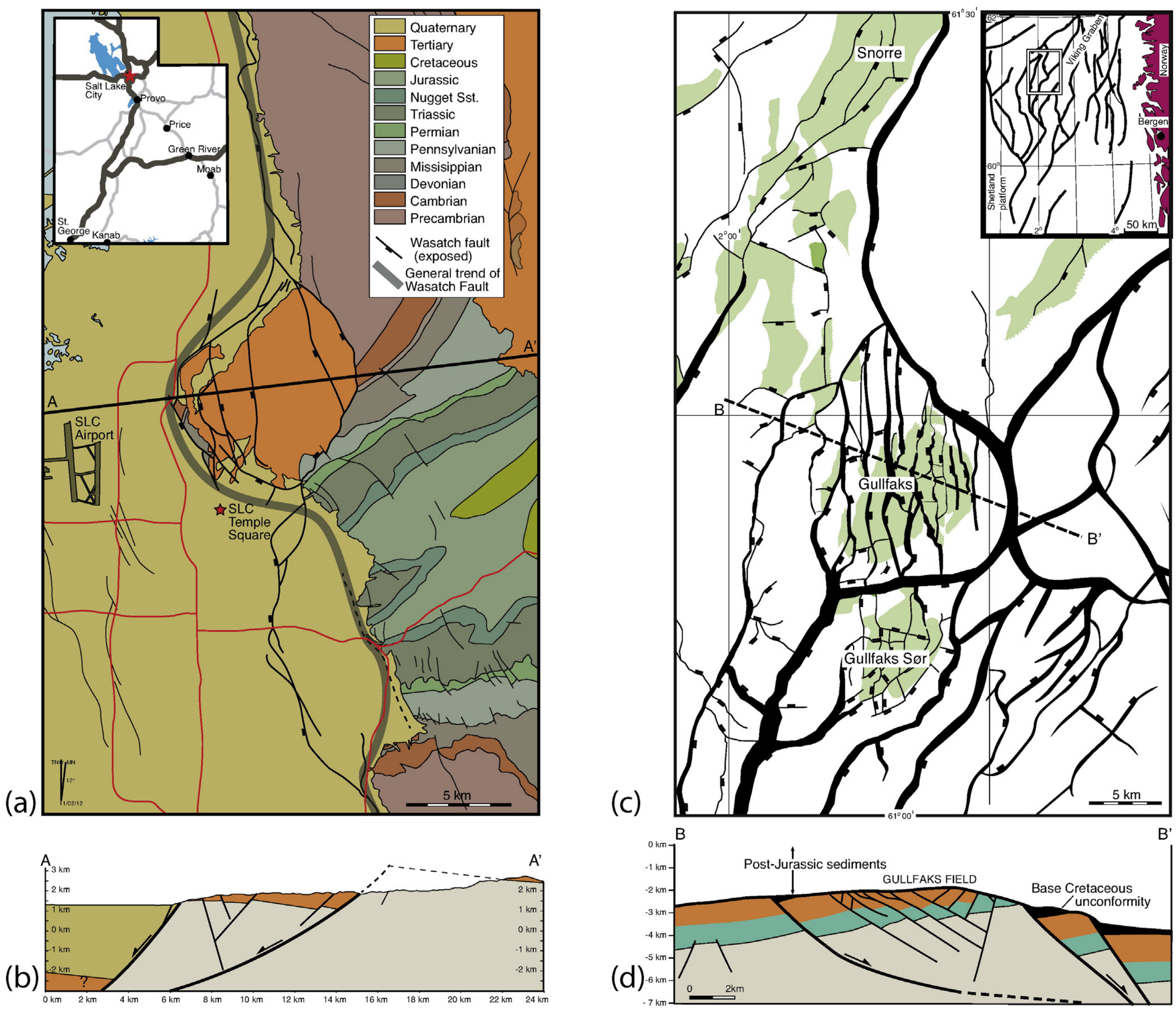

Fig. 14. Structural maps and cross-sections of the Salt Lake (a–b) and Gullfaks (c–d) salients. Geometrically the two areas are almost mirror images of each other, and we propose that both formed as a result of fault linkage.

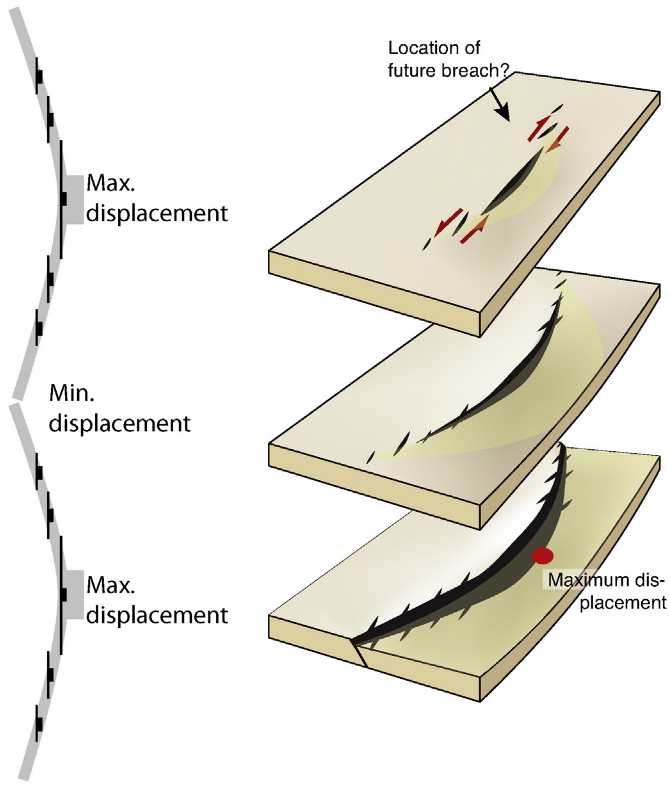

Fig. 15. The formation of curved faults (in map view) according to the model suggested by Wu and Bruhn (1994). The shear component in the tip regions of active faults causes the fault to step out of its own plane in the sense shown in the figure, thereby causing a curved fault trace as the segments link up to a continuous fault surface.

expected where the salient parts of large fault blocks are tilted and where footwall uplift is prominent. Gravitational sliding near the surface will be the most obvious effect, but if the salient and fault block are large enough it may also have an effect on the deeper parts of the system. A characteristic feature of both the Salt Lake and the Gullfaks salients is the formation of subsidiary ("shortcut") faults that transect the salients, transferring some of the displacement more directly between the main fault segments (Fig. 14).

A different model for curved fault traces employs the fact that lateral shear (strike–slip) components occur in the lateral tip regions of a normal fault because hanging-wall subsidence greatly exceeds footwall uplift (Wu and Bruhn, 1994; Roberts, 1996). It has been suggested that this asymmetry may generate en-échelon faults ahead of the fault tips in map view. Since, in accordance with the sense of shear in the tip regions, the fault will step into the footwall, the result may be a curved fault as these fault segments link up, as shown in Fig. 15 (Wu and Bruhn, 1994). This model implies that the point of maximum displacement occurs in the salients or convex parts of the curved faults (Fig. 15), which makes for a simple test. While this model does not seem to apply to the Wasatch and Gullfaks faults (Fig. 14), Wu and Bruhn (1994) suggest that the geometric pattern of the South Oquirrh Mountains normal fault zone fits this model.

4. Consequences for fluid flow

Relay ramps, breached or not, typically represent potential pathways for vertical migration of fluids (Fig. 16). The reason for this is the increased structural complexity found at fault relays, with increased numbers of faults and fractures and a wider range of orientations than that of single, isolated faults (e.g. Sibson, 1996; Peacock and Parfitt, 2002; Kim et al., 2004; Fossen et al., 2005). Relay zones therefore represent an important control on fluid transport in the crust, affecting all kinds of fluids, including hydrocarbons, CO_2 and other volatiles, hydrothermal solutions, metamorphic fluids, magma, and ground water. Relay zones are therefore the loci of a range of fluid–rock interactive processes, many of which are of economic significance. One such example is provided in a study of a segmented rift system in New Zealand by Rowland and Sibson (2004), where a concentration of geothermal fields in fault stepovers were identified, and linked to enhanced vertical permeability caused by high structural complexity in these zones. Evidence for increased geothermal fluid activity linked to fault linkage zones was also reported by Curewitz and Karson (1997), and by Dockrill and Shipton (2010) who showed that CO_2 springs and seeps were co-located with structurally complex zones in a fault array. Also in volcanic systems, magma emplacement has been correlated with dilational jogs or transverse fault relays (Vigneresse and Bouchez, 1997) and extensional transfer zones (Dini et al., 2008). Also in association with magmatism, where hydrothermal activity is high, economically important hydrothermal mineral deposits may be related to fault relays or intersections. As an example, copper mineralization along the Lisbon Valley Fault and the Dolores Zone of faults in Utah and Colorado (Breit and Meunier, 1990) are localized at relay zones. Furthermore, fault jogs, which commonly represent the locations of previous fault linkage zones, have been shown to be associated with hydrothermal gold deposits in strike-slip systems (Micklethwaite and Cox, 2004, 2006).

Due to the ability of the fault relay zones to control fluid transport, and therefore the loci of fluid–rock interaction, fault relays may also exercise strong control on diagenesis. For example, Eichhubl et al. (2009) showed that fluid migration and cementation along the Moab Fault (Utah) was focused at areas of fault linkage or intersection. Another example is presented by Sharp et al. (2010), where dolomitization of Cretaceous carbonates in the Zagros Mountains of Iran have been subject to strong structural controls; particularly, the authors note that alteration is most extensive at faults/joint intersections.

Fault relays and intersections are also important for the accumulation and retainment of hydrocarbons. They may act as vertical conduits for fluid migration into traps but may also have negative effect on seal

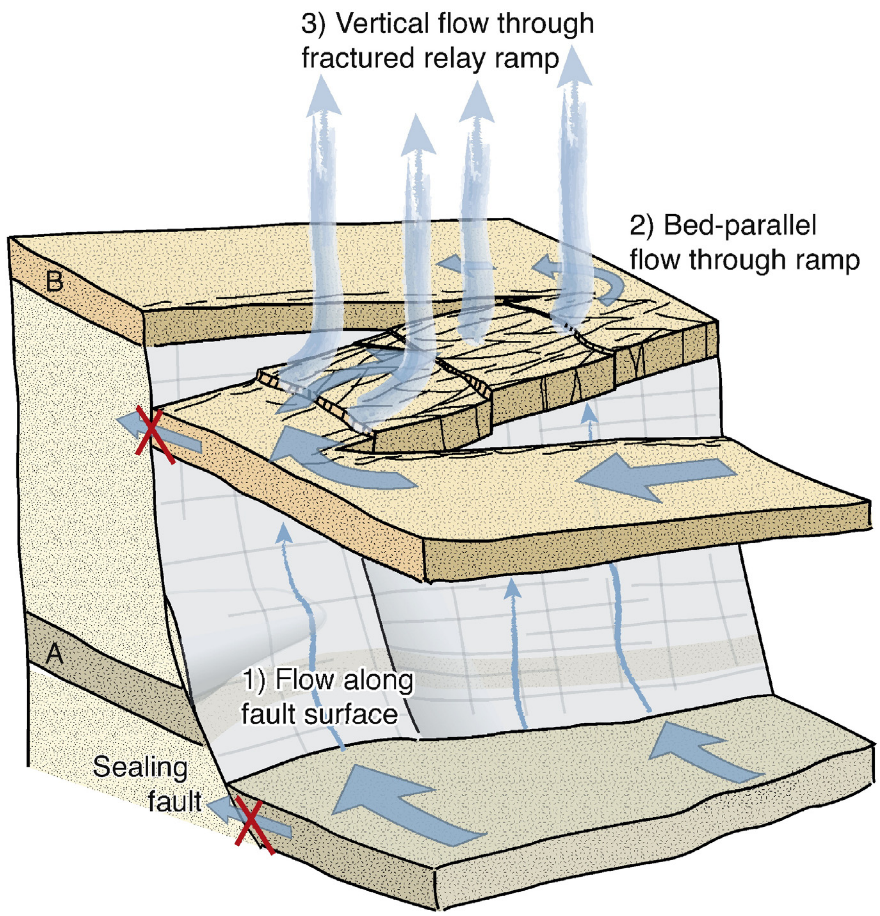

Fig. 16. Fluid flow-pattern through a relay structure (layer A). A sealing fault may conduct fluids in the vertical direction (1), but much more efficiently so through a heavily fractured relay structure (3). In a reservoir setting the relay structure typically provide bed-parallel hanging-wall–footwall communication (2). Layer B does not show a ramp geometry and is not associated with flow of types 2 and 3.

integrity. In a study of petroleum fields in the Timor Sea, Australia, Gartrell et al. (2004) identified fault intersections as critical hydrocarbon leakage zones. This is also supported by findings by Kristiansen (2011), who found that for fault-controlled structural hydrocarbon traps in the Barents Sea (Norway), traps were generally *underfilled or dry* where controlled by *two or more interacting faults*, whereas all *discoveries* were associated with fault traps controlled by a *single fault*.

In addition to these aspects relevant for hydrocarbon exploration, fault relay zones may also affect fluid flow between structural reservoir compartments on a production time scale. Soft-linked relay zones may offer cross-fault reservoir connectivity through folded but unbreached relay beds (Bense and Baalen, 2004; Manzocchi et al., 2008; Rotevatn et al., 2009a). However, this effect may be reduced if the relay zone is associated with a linking damage zone of low-permeable deformation bands in porous sandstone host rocks (Rotevatn et al., 2009b, Rotevatn and Fossen, 2011). Another way that relay zones may aid cross-fault fluid flow is the juxtaposition of multiple reservoir units at different stratigraphic levels due to folded beds and steep displacement gradients (Manzocchi et al., 2010, their fig. 12).

In non-porous rocks, where fractures comprise most of the permeability, bed continuity in itself through a relay zone may have limited effect on cross-fault flow. However, greater density and variety in orientation of the permeability-controlling fractures may aid also cross-fault flow. Along isolated fault segments, high-permeablity fracture systems and fault slip surfaces generally have a positive effect on fault-parallel permeability, but the effect on cross-fault permeability is limited (Jourde et al., 2002) as most fractures are oriented subparallel to the fault. In relay zones, however, increased fracture intensity and orientation variability in the linking damage zone leads to an increased fracture:matrix ratio and connectivity, both of which lead to a higher overall effective permeability (e.g. Berkowitz, 1995). Adding to this is the fact that, when there is a great range in orientation, the chance of some of the fractures being optimally oriented for opening is great under most stress conditions. Rotation of the local stress field, which is common in relay zones (Kattenhorn et al., 2000) may lead to principal stress orientations which, if oriented optimally with respect to fractures, may promote greater fracture apertures that increase permeability (e.g. Tamagawa and Pollard, 2008). Relevant to this, drilling of active fault systems demonstrated that, although a small percentage of fault-related fractures only may be optimally oriented for opening under the regional stress regime, these maintain the largest hydraulic conductivities at any given time (Barton et al., 1995; Davatzes and Hickman, 2005). Dilatant stress conditions at vertical and lateral fault jogs or intersections have also previously been suggested (e.g. Ferrill and Morris, 2003, Gartrell et al., 2004), and have important implications for the permeability structure at such locations.

Relay-enhanced fault permeability should also be considered in a temporal perspective. Whereas intact relays may provide cross-fault connectivity in porous sandstones, a breached relay in such rocks will represent a zone of enhanced low-permeable damage in the form of deformation bands, in addition to the breaching fault itself. In such rocks, cross-fault permeability may therefore be increased in the presence of a soft-linked relay (Rotevatn et al., 2009b), but reduced in the presence of a breached relay. This contrasts findings in fractured carbonate reservoir rocks (Bastesen and Rotevatn, 2012, Rotevatn and Bastesen, 2012), where it was shown that breached relays in

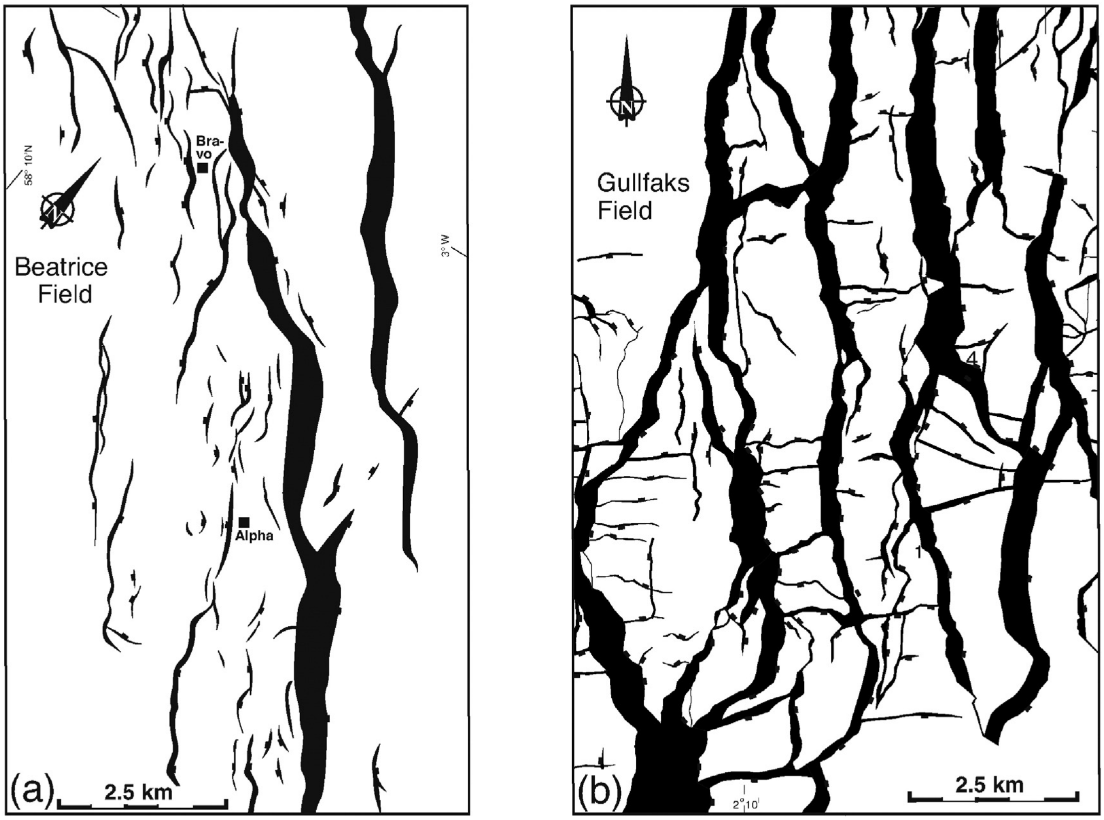

Fig. 17. Two fault maps from the North Sea, showing the fault pattern of the Beatrice Field (Inner Moray Firth basin) and that of the structurally more mature Gullfaks Field. Note how faults are longer and better connected in the Gullfaks Field, where multiple previous relays can be inferred from kinks and jogs in the fault traces. The highly compartmentalized Gullfaks Field requires many wells for efficient production while fewer wells are needed to produce the Beatrice Field with its well-connected fault blocks. Based on Husmo et al. (2002) and Fossen (2010).

such rocks may provide better cross-fault connectivity compared to soft-linked relays. The reason for this is that in such rocks, fracture system development and permeability enhancement was found to progress during continual relay growth and linkage, and to be greatest at breached relays.

A consequence of fault growth through linkage is the development of long and continuous faults at advanced stages. As relay ramps form and breach, these long faults compartmentalize reservoirs and may produce long and isolated fault blocks that act as individual fluid compartments. The linkage and breaching of relays leads to more connected fault systems, and a relationship between strain and fault population maturity exists. The Gullfaks Field in the northern North Sea (Fossen and Hesthammer, 1998) may serve as an example of a structurally mature fault system where high degree of fault connectivity and structural complexity has required a high number of production and injection wells (Fig. 17). The strain in the part of the Gullfaks Field shown in Fig. 17b is more than 40%, approximately twice that of the structurally less mature fault array of the Beatrice field shown in Fig. 17a.

5. Concluding remarks

The formation of relay structures during the development of normal fault populations is extremely common, from the cm-scale to tens of kilometers in width. They portray geometric properties that appear to be scale independent, including their shape (3–3.5 times longer than their width) and the displacement variations along overlapping fault tips and therefore ramp geometry. Typically the steepness of ramps at the point of breaching is around 10–15°, and the breaching process itself results in a wide and complicated zone of damage that is largely inactivated after breaching. These damage zones may have different functionality with respect to fluid flow, depending on the properties of the structural elements of which they are constituted. While their tendency to reduce lateral fluid flow within many sandstone reservoirs is well known, their possible role as vertical conduits is less explored. Particular attention should be paid to this aspect during planning and monitoring of CO_2 sequestration and hydrocarbon exploration/production alike.

More detailed work is needed to understand the variability of ramp evolution and destruction. Detailed geometric analysis of ramps at various scales and settings are needed to relate geometry (dip, curvature) to small-scale damage and to location of breaching. The influence of three-dimensional fault geometry on ramp development is also needed: ramps are commonly considered at a single stratigraphic level only, while true fault geometry may have important bearings on their development.

Acknowledgments

We are grateful for careful and constructive reviews by George Hilley and editor Manfred Strecker.

References

Ackermann, R.V., Schlische, R.W., 1997. Anticlustering of small normal faults around larger faults. Geology 25, 1127–1130.
Acocella, V., Gudmundsson, A., Funiciello, R., 2000. Interaction and linkage of extension fractures and normal faults: examples from the rift zone of Iceland. J. Struct. Geol. 22, 1233–1246.
Allken, V., Huismans, R.S., Fossen, H., Thieulot, C., 2013. 3D numerical modelling of graben interaction and linkage: a case study of the Canyonlands grabens, Utah. Basin Res. 25, 14.
Anders, M.H., Schlische, R.W., 1994. Overlapping faults, intrabasin highs, and the growth of normal faults. J. Geol. 102, 165–180.
Anderson, E.M., 1951. The Dynamics of Faulting. Oliver & Boyd, Edinburgh.

Antonellini, M.A., Aydin, A., Pollard, D.D., 1994. Microstructure of deformation bands in porous sandstones at Arches National Park, Utah. J. Struct. Geol. 16, 941–959.

Athmer, W., Groenenberg, R.M., Luthi, S.M., Donselaar, M.E., Sokoutis, D., Willingshofer, E., 2010. Relay ramps as pathways for turbidity currents: a study combining analogue sandbox experiments and numerical flow simulations. Sedimentology 57, 806–823.

Aydin, A., Borja, R.I., Eichhubl, P., 2006. Geological and mathematical framework for failure modes in granular rock. J. Struct. Geol. 28, 83–98.

Barton, C.A., Zoback, M.D., Moos, D., 1995. Fluid flow along potentially active faults in crystalline rock. Geology 23, 683–686.

Bastesen, E., Rotevatn, A., 2012. Evolution and structural style of relay zones in layered limestone–shale sequences: insights from the Hammam Faraun Fault Block, Suez Rift, Egypt. Geol. Soc. Lond. 169, 477–488.

Bense, V.F., Baalen, R.V., 2004. The effect of fault relay and clay smearing on groundwater flowpatterns in the Lower Rhine Embayment. Basin Res. 16, 397–411.

Bergner, A.G.N., Strecker, M.R., Trauth, M.H., Deino, A.L., Gasse, F., Blisniuk, P., Dünforth, M., 2009. Tectonic and climatic control on evolution of rift lakes in the Central Kenya Rift, East Africa. Quat. Sci. Rev. 28, 2804–2816.

Berkowitz, B., 1995. Analysis of fracture network connectivity using percolation theory. Math. Geol. 27, 467–483.

Bosworth, W., 1985. Geometry of propagating continental rifts. Nature 316, 625–627.

Bosworth, W., 1987. Off-axis volcanism in the Gregory rift, east Africa: implications for models of continental rifting. Geology 15, 397–400.

Bosworth, W., 2015. Geological Evolution of the Red Sea: Historical Background, Review, and Synthesis. pp. 45–78.

Bott, M.H.P., 1959. The mechanics of oblique slip faulting. Geol. Mag. 46, 110–117.

Breit, G.N., Meunier, J., 1990. Fluid inclusion, d18O, and 87Sr/86Sr evidence for the origin of fault-controlled copper mineralization, Lisbon Valley, Utah, and Slick Rock District, Colorado. Econ. Geol. 85, 884–891.

Cartwright, J.A., Mansfield, C.S., 1998. Lateral displacement variation and lateral tip geometry of normal faults in Canyonlands National Park, Utah. J. Struct. Geol. 20, 3–19.

Childs, C., Manzocchi, T., Walsh, J.J., Bonson, C.G., Nicol, A., Schöpfer, M.P.J., 2009. A geometric model of fault zone and fault rock thickness variations. J. Struct. Geol. 31, 117–127.

Coney, P.J., Harms, T.A., 1984. Cordilleran metamorphic core complexes: Cenozoic extensional relics of Mesozoic compression. Geology 12, 550–555.

Cowie, P., Roberts, G.P., 2001. Constraining slip rates and spacings for active normal faults. J. Struct. Geol. 23, 1901–1915.

Cowie, P., Gupta, S., Dawers, N.H., 2000. Implications of fault array evolution for synrift depocentre development: insights from a numerical fault growth model. Basin Res. 12, 241–261.

Cox, S.F., 2005. Coupling between deformation, fluid pressures, and fluid flow in ore-producing hydrothermal systems at depth in the crust. Econ. Geol. 100th Anniversary, 39–76.

Crider, J.G., Pollard, D.D., 1998. Fault linkage: three-dimensional mechanical interaction between echelon normal faults. J. Geophys. Res. 103, 675–692.

Curewitz, D., Karson, J.A., 1997. Structural settings of hydrothermal outflow: fracture permeability maintained by fault propagation and interaction. J. Volcanol. Geotherm. Res. 79, 149–168.

Dahlstrom, C.D.A., 1969. Balanced cross sections. Can. J. Earth Sci. 6, 743–757.

Davatzes, N.C., Hickman, S.H., 2005. Controls on fault-hosted fluid flow; Preliminary results from the Coso geothermal field. Geothermal Research Council Transactions, paper, CA, p. 144.

Delaney, P.T., Pollard, D.D., 1981. Deformation of host rocks and flow of magma during growth of minette dikes and breccia-bearing intrusions near Ship Rock, New Mexico. USGS Professional Paper 1202 (61 pp.).

Destro, N., Alkmim, F.F., Magnavita, L.P., Szatmari, P., 2003. The Jeremoabo transpressional transfer fault, recôncavo–Tucano rift, NE Brazil. J. Struct. Geol. 25, 1263–1279.

Dini, D.S.W., Innocenti, F., Rocchi, S., 2008. Magma emplacement in a transfer zone: the Miocene mafic Orano dyke swarm of Elba Island, Tuscany, Italy. Geol. Soc. Lond. Spec. Publ. 302, 131–148. http://dx.doi.org/10.1144/SP302.10.

Dockrill, B., Shipton, Z.K., 2010. Structural controls on leakage from a natural CO_2 geologic storage site: Central Utah, U.S.A. J. Struct. Geol. 32.

Duval, B., Cramez, C., Jackson, M.P.A., 1992. Raft tectonics in the Kwanza Basin, Angola. Mar. Pet. Geol. 9, 389–390.

Eichhubl, P., Davatzes, N.C., Becker, S.P., 2009. Structural and diagenetic control of fluid migration and cementation along the Moab fault, Utah. Am. AAPG Bull. 93, 653–681.

Elliott, G.M., Wilson, P., Jackson, C.A.L., Gawthorpe, R.L., Michelsen, L., Sharp, I.R., 2011. The linkage between fault throw and footwall scarp erosion patterns: an example from the Bremstein Fault Complex, offshore Mid-Norway. Basin Res. 23, 1–18.

Færseth, R.B., 1996. Interaction of Permo-Triassic and Jurassic extensional fault-blocks during the development of the northern North Sea. J. Geol. Soc. 153, 931–944.

Faulds, J.E., Varga, R.J., 1998. The role of accommodation zones and transfer zones in the regional segmentation of extended terranes. Geol. Soc. Am. Spec. Paper 323 (45 pp.).

Faulds, J.E., Hinz, N.H., Dering, G.M., Siler, D.L., 2013. The hybrid model —the most accommodating structural setting for geothermal power generation in the Great Basin, Western USA. GRC Trans. 37, 3–10.

Ferrill, D.A., Morris, A.P., 2001. Displacement gradient and deformation in normal fault systems. J. Struct. Geol. 23, 619–638.

Ferrill, D.A., Morris, A.P., 2003. Dilational normal faults. J. Struct. Geol. 25, 183–196.

Finzi, Y., Langer, S., 2012. Damage in step-overs may enable large cascading earthquakes. Geophys. Res. Lett. http://dx.doi.org/10.1029/2012GL052436 (5 pp.).

Fort, X., Brun, J.P., Chauvel, F., 2004. Salt tectonics on the Angolan margin, synsedimentary deformation processes. AAPG Bull. 88, 1523–1544.

Fossen, H., 2010. Structural Geology. Cambridge University Press (463 pp.).

Fossen, H., Hesthammer, J., 1998. Structural geology of the Gullfaks Field, northern North Sea. Geol. Soc. Lond. Spec. Publ. 127, 231–261.

Fossen, H., Johansen, T.E.S., Hesthammer, J., Rotevatn, A., 2005. Fault interaction in porous sandstone and implications for reservoir management; examples from Southern Utah. AAPG Bull. 89, 1593–1606.

Fossen, H., Odinsen, T., Færseth, R.B., Gabrielsen, R.H., 2000. Detachments and low-angle faults in the northern North Sea rift system. Geol. Soc. Lond. Spec. Publ. 167, 105–131.

Fossen, H., Schultz, R.A., Rundhovde, E., Rotevatn, A., Buckley, S., 2010. Fault linkage and graben stepovers in the Canyonlands (Utah) and the North Sea Viking Graben, with implications for hydrocarbon migration and accumulation. AAPG Bull. 94, 597–613.

Fossen, H., Schultz, R.A., Shipton, Z.K., Mair, K., 2007. Deformation bands in sandstone—a review. Geol. Soc. Lond. 164, 755–769.

Gartrell, A., Zhang, Y., Lisk, M., Dewhurst, D., 2004. Fault intersections as critical hydrocarbon leakage zones: integrated field study and numerical modelling of an example from the Timor Sea, Australia. Mar. Pet. Geol. 21, 1165–1179.

Gawthorpe, R.L., Hurst, J.M., 1993. Transfer zones in extensional basins: their structural style and influence on drainage development and stratigraphy. Geol. Soc. Lond. 150, 1137–1152.

Gawthorpe, R., Leeder, M.R., 2000. Tectono-sedimentary evolution of active extensional basins. Basin Res. 12, 195–218.

Giba, M., Walsh, J.J., Nicol, A., 2012. Segmentation and growth of an obliquely reactivated normal fault. J. Struct. Geol. 39, 253–267.

Gibbs, A.D., 1984. Structural evolution of extensional basin margins. Geol. Soc. Lond. 141, 609–620.

Goguel, J., 1952. Traité de Tectonique. Masson, Paris.

Gupta, A., Scholz, C.H., 2000. A model of normal fault interaction based on observations and theory. J. Struct. Geol. 22, 865–879.

Hetzel, R., Strecker, R., 1994. Late Mozambique Belt structures in western Kenya and their influence on the evolution of the Cenozoic Kenya Rift. J. Struct. Geol. 2, 189–201.

Huggins, P., Watterson, J., Walsh, J.J., et al., 1995. Relay zone geometry and displacement transfer between normal faults recorded in coal-mine plans. J. Struct. Geol. 17, 1741–1755.

Lower and middle Jurassic. In: Husmo, T., Hamar, G.P., Høiland, O., Johannesen, E.P., Rømuld, A., Spencer, A.M., Tritterton, R. (Eds.), The Millennium Atlas: Petroleum Geology of the Central and Northern North Sea. Geol. Soc., London, pp. 129–155.

Jackson, C.A.L., Rotevatn, A., 2013. 3D seismic analysis of the structure and evolution of a salt-influenced normal fault zone: a test of competing fault growth models. J. Struct. Geol. 53. http://dx.doi.org/10.1016/j.jsg.2013.06.012.

Jackson, C.A.L., Gawthorpe, R., Sharp, I.R., 2002. Growth and linkage of the East Tanka fault zone, Suez rift: structural style and syn-rift stratigraphic response. J. Geol. Soc. 159, 175–187.

Jourde, H., Flodin, E.A., Aydin, A., Durlofsky, et al., 2002. Computing permeabilities of fault zones in eolian sandstone from outcrop measurements. AAPG Bull. 86, 1187–1200.

Kattenhorn, S.A., Aydin, A., Pollard, D.D., 2000. Joints at high angles to normal fault strike: an explanation using 3-D numerical models of fault-perturbed stress fields. J. Struct. Geol. 22, 1–23.

Kim, Y.-S., Peacock, D.C.P., Sanderson, D.J., 2004. Fault damage zones. J. Struct. Geol. 26, 503–517.

Kinabo, B.D., Atekwana, E.A., Hogan, J.P., Modisi, M.P., Wheaton, D.D., Kampunzu, A.B., 2007. Early structural development of the Okavango rift zone, NW Botswana. J. Afr. Earth Sci. 48, 125–136.

Kristensen, M.B., Childs, C., Olesen, N.Ø., Korstgård, J.A., 2013. The microstructure and internal architecture of shear bands in sand–clay sequences. J. Struct. Geol. 46, 129–141.

Kristiansen, K., 2011. Vertical fault leakage in the western part of the Hammerfest Basin. Unpublished MSc thesis, University of Bergen, (94 pp.)

Larsen, P.-H., 1988. Relay structures in a Lower Permian basement-involved extension system, East Greenland. J. Struct. Geol. 10, 3–8.

Long, J.J., Imber, J., 2011. Geological controls on fault relay zone scaling. J. Struct. Geol. 33, 1790–1800.

Machette, M.N., Personius, S.F., Nelson, A.R., Schwartz, D.P., Lund, W.R., 1991. The Wasatch fault zone, Utah—segmentation and history of Holocene earthquakes. J. Struct. Geol. 13, 137–149.

Maerten, L., Willemse, E.J.M., Pollard, D.D., et al., 1999. Slip distributions on intersecting normal faults. J. Struct. Geol. 21, 259–271.

Manighetti, I., Zigone, D., Campillo, M., Cotton, F., 2009. Self-similarity of the largest-scale segmentation of the faults: implications for earthquake behavior. Earth Planet. Sci. Lett. 288, 370–381.

Manzocchi, T., Childs, C., Walsh, J.J., 2010. Faults and fault properties in hydrocarbon flow models. Geofluids 10, 94–113.

Manzocchi, T., Heath, A.E., Palananthakumar, B., Childs, C., Walsh, J.J., 2008. Faults in conventional flow simulation models: a consideration of representational assumptions and geological uncertainties. Pet. Geosci. 14, 91–110.

McClay, K.R., Ellis, P.G., 1987. Analogue models of extensional fault geometries. Geol. Soc. Lond. Spec. Publ. 28, 109–125.

Micklethwaite, S., Cox, S.F., 2004. Fault-segment rupture, aftershock-zone fluid flow, and mineralization. Geology 32, 813.

Micklethwaite, S., Cox, S., 2006. Progressive fault triggering and fluid flow in aftershock domains: examples from mineralized Archaean fault systems. Earth Planet. Sci. Lett. 250, 318–330.

Milani, E.J., Davison, I., 1988. Basement control and transfer tectonics in the Recôncavo–Tucano–Jatobá rift, Northeast Brazil. Tectonophysics 154, 41–70.

Morellato, C., Redini, F., Doglioni, C., 2003. On the number and spacing of faults. Terra Nova 15, 315–321.

Morley, C.K., Nelson, R.A., Patton, T.L., Munn, S.G., 1990. Transfer zones in the East African rift system and their relevance to hydrocarbon exploration in rifts. AAPG Bull. 74, 1234–1253.
Nicol, A., Gillespie, P., Childs, C., Walsh, J.J., 2002. Relay zones between mesoscopic thrust faults in layered sedimentary sequences. J. Struct. Geol. 24, 709–727.
Nicol, A., Watterson, J., Walsh, J.J., Gillespie, P.A., 1996. The shapes, major axis orientations and displacement patterns of fault surfaces. J. Struct. Geol. 18, 235–248.
Peacock, D.C.P., Parfitt, E.A., 2002. Active relay ramps and normal fault propagation on Kilauea Volcano, Hawaii. J. Struct. Geol. 24, 729–742.
Peacock, D.C.P., Sanderson, D.J., 1991. Displacements, segment linkage and relay ramps in normal fault zones. J. Struct. Geol. 13, 721–733.
Peacock, D.C.P., Price, S.P., Pickles, C.S., 2000. The world's biggest relay ramp: hold with hope, NE Greenland. J. Struct. Geol. 22, 843–850.
Podolsky, D.M.W., Roberts, G.P., 2008. Growth of the volcano-flank Koa'e fault system, Hawaii. J. Struct. Geol. 30 (10), 1254–1263.
Roberts, G.P., 1996. Variation in fault-slip directions along active and segmented normal fault systems. J. Struct. Geol. 18, 835–845.
Rosendahl, B.R., Reynolds, D.J., Lorber, Burgess, C.F., McGill, J., Scott, D., Lambiase, J.J., Derksen, S.J., 1986. Structural expressions of rifting: lessons from Lake Tanganykia, Africa. Geol. Soc. Lond. Spec. Publ. 25, 29–43.
Rotevatn, A., Bastesen, E., 2012. Fault linkage and damage zone architecture in tight carbonate rocks in the Suez Rift (Egypt): implications for permeability structure along segmented normal faults. Geol. Soc. Lond. Spec. Publ. 374. http://dx.doi.org/10.1144/SP374.12.
Rotevatn, A., Fossen, H., 2011. Simulating the effect of subseismic fault tails and process zones in a siliciclastic reservoir analogue: implications for aquifer support and trap definition. Mar. Pet. Geol. 28, 1648–1662.
Rotevatn, A., Buckley, S.J., Howell, J.A., Fossen, H., 2009a. Overlapping faults and their effect on fluid flow in different reservoir types: a LIDAR-based outcrop modeling and flow simulation study. AAPG Bull. 93, 407–427.
Rotevatn, A., Fossen, H., Hesthammer, J., 2007. Are relay ramps conduits for fluid flow? Structural analysis of a relay ramp in Arches National Park, Utah. Geol. Soc. Lond. Spec. Publ. 270, 55–71.
Rotevatn, A., Tveranger, J., Howell, J.A., 2009b. Dynamic investigation of the effect of a relay ramp on simulated fluid flow: geocellular modelling of the Delicate Arch Ramp, Utah. Pet. Geosci. 15, 45–58.
Rouby, D., Nalpas, T., Jermannaud, P., 2011. Gravity driven deformation controlled by the migration of the delta front: the Plio-Pleistocene of the Eastern Niger Delta. Tectonophysics 513, 54–67.
Rowland, J.V., Sibson, R.H., 2004. Structural controls on hydrothermal flow in a segmented rift system, Taupo Volcanic Zone, New Zealand. Geofluids 4, 259–283.
Schlische, R.W., Withjack, M.O., 2009. Origin of fault domains and fault-domain boundaries (transfer zones and accommodation zones) in extensional provinces: result of random nucleation and self-organized fault growth. J. Struct. Geol. 31, 910–925.
Schwartz, D.P., Coppersmith, K.J., 1984. Fault behavior and characteristic earthquakes: examples from the Wasatch and San Andreas Fault Zones. J. Geophys. Res. 89 (B7), 5681.
Scott, D.L., Rosendahl, B.R., 1989. North Viking Graben: an east African perspective. AAPG Bull. 73, 155–165.
Sharp, I., Gillespie, P., Morsalnezhad, D., Taberner, C., Karpuz, R., Verge, S.,J., Horbury, A., Pickard, N., Garland, J., Hunt, D., 2010. Stratigraphic architecture and fracture-controlled dolomitization of the Cretaceous Khami and Bangestan groups: an outcrop case study, Zagros Mountains, Iran. Geol. Soc. Spec. Publ. 329, 343–396.
Sibson, R.H., 1996. Structural permeability of fluid-driven fault-fracture meshes. J. Struct. Geol. 18, 1031–1042.
Smith, M., Mosley, P., 1993. Crustal heterogeneity and basement influence on the development of the Kenya Rift, East Africa. Tectonics 12, 591–606.
Soliva, R., Benedicto, A., 2004. A linkage criterion for segmented normal faults. J. Struct. Geol. 26, 2251–2267.
Soliva, R., Schultz, R.A., 2008. Distributed and localized faulting in extensional settings: insight from the North Ethiopian Rift–Afar transition area. Tectonics 27. http://dx.doi.org/10.1029/2007TC002148 (19 pp.).
Soliva, R., Benedicto, A., Maerten, L., 2006. Spacing and linkage of confined normal faults: importance of mechanical thickness. J. Geophys. Res. 111 (B1), 17p. http://dx.doi.org/10.1029/2004JB003507.
Spadini, G., Podladchikov, Y., 1996. Spacing of consecutive normal faulting in the lithosphere: a dynamic model for rift axis jumping (Tyrrhenian Sea). Earth Planet. Sci. Lett. 144, 21–34.
Tamagawa, T., Pollard, D.D., 2008. Fracture permeability created by perturbed stress fields around active faults in a fractured basement reservoir. AAPG Bull. 92, 743–764.
Tentler, T., Mazzoli, S., 2005. Architecture of normal faults in the rift zone of central north Iceland. J. Struct. Geol. 27, 1721–1739.
Trudgill, B., Cartwright, J., 1994. Relay-ramp forms and normal-fault linkages, Canyonlands National Park, Utah. Geol. Soc. Am. Bull. 106, 1143–1157.
Vendeville, B., Cobbold, P.R., 1988. How normal faulting and sedimentation interact to produce listric fault profiles and stratigraphic wedges. J. Struct. Geol. 10, 649–659.
Vendeville, B., Cobbold, P.R., Davy, P., Brun, J.P., Choukroune, P., 1987. Physical models of extensional tectonics at various scales. Geol. Soc. Lond. Spec. Publ. 28, 95–107.
Vigneresse, J.L., Bouchez, J.L., 1997. Successive granitic magma batches during pluton emplacement: the Case of Cabeza de Araya (Spain). J. Petrol. 38, 1767–1776.
Walsh, J.J., Watterson, J., 1991. Geometric and kinematic coherence and scale effects in normal fault systems. Geol. Soc. Lond. Spec. Publ. 56, 193–203.
Walsh, J.J., Bailey, W.R., Childs, et al., 2003. Formation of segmented normal faults: a 3-D perspective. J. Struct. Geol. 25, 1251–1262.
Wernicke, B., Burchfiel, B.C., 1982. Modes of extensional tectonics. J. Struct. Geol. 4, 105–115.
Willemse, E.J.M., 1997. Segmented normal faults: correspondence between three-dimensional mechanical models and field data. J. Geophys. Res. 1902, 675–692.
Willemse, E.J.M., Pollard, D.D., Aydin, A., 1996. Three-dimensional analyses of slip distributions on normal fault arrays with consequences for fault scaling. J. Struct. Geol. 18, 295–309.
Wu, D., Bruhn, R.L., 1994. Geometry and kinematics of active normal faults, South Oquirrh Mountains, Utah: implication for fault growth. J. Struct. Geol. 16, 1061–1075.
Wu, J.E., McClay, K., Frankowicz, E., 2015. Niger Delta gravity-driven deformation above the relict Chain and Charcot oceanic fracture zones, Gulf of Guinea: insights from analogue models. Mar. Pet. Geol. 65, 43–62.
Xiao-shuang, X., Jing-ru, T., Hua, K., Shao-xun, H., 2005. Control of relay structure on mineralization of sedimentary-exhalative ore deposit in growth faults of graben systems. J. Cent. S. Univ. Technol. 12, 340–345.
Xu, S., Nieto-Samaniego, A.F., Alaniz-Alvarez, S.A., et al., 2011. Structural analysis of a relay ramp in the Querétaro graben, central Mexico: implications for relay ramp development. Rev. Mex. Cienc. Geol. 28, 275–289.
Younes, A.I., McClay, K., 2002. Development of accommodation zones in the Gulf of Suez–Red Sea rift, Egypt. AAPG Bull. 86, 1003–1026.
Young, M.J., Gawthorpe, R.L., Hardy, S., 2001. Growth and linkage of a segmented normal fault zone; the Late Jurassic Murchison–Statfjord North Fault, northern North Sea. J. Struct. Geol. 23, 1933–1952.